Easterly Waves over Africa. Part II: Observed and Modeled Contrasts between Wet and Dry Years

Jeremy P. Grist* and Sharon E. Nicholson

Department of Meteorology, The Florida State University, Tallahassee, Florida

Albert I. Barcilon

Geophysical Fluid Dynamics Institute, The Florida State University, Tallahassee, Florida

ABSTRACT

Differences in the basic state over West Africa between wet and dry years are well documented. This study investigates whether there are also observable differences in the easterly waves between wet and dry years and if these differences might be attributed to the changes in the basic state.

Contrasting basic states from the rainy seasons of the four wet years (1958–61) and four dry years (1982–85) were derived from the NCEP reanalysis. The basic states served as input for the linear instability model. The model results indicated faster growth rates and greater phase speeds in the wet years. These results were consistent with a wavelet analysis of the 600-mb meridional wind. This analysis showed that waves were stronger and tended to have a greater contribution from the longer periods during the wet years.

The differences in the waves appear to be due to the greater horizontal and vertical shear in wet years. The relative importance of these two were assessed using the Charney–Stern necessary condition for instability. It appears that the horizontal shear is more important in causing the differences. Although the baroclinic and barotropic terms were of similar magnitude in dry years, in wet years the barotropic term increased significantly, whereas the baroclinic term did not. Implications of the results for the understanding of interannual and interdecadal rainfall variability over West Africa are discussed.

1. Introduction

During the past two decades our understanding of the meteorology of West Africa has dramatically increased as a result of the Global Atmospheric Research Program (GARP) Atlantic Tropical Experiment (GATE) in 1974 and as a result of studies prompted by the protracted drought that has prevailed since the late 1960s. Previously, a simple scenario was assumed in which the rainy season was a consequence of localized storms associated with the intertropical convergence zone (ITCZ) and its seasonal migration. The picture of regional dynamics that has since emerged is radically different. It is now accepted, for example, that the midtropospheric African easterly jet (AEJ) plays a more important role than the ITCZ and that the rain-bearing disturbances are generally linked to well-organized mesoscale features.

These features appear to be associated with African easterly waves (AEWs), the development of which Burpee (1972, 1974) and others have shown to be dynamically linked to the AEJ. It is well known that the waves tend to organize rainfall into the mesoscale systems (e.g., Reeves et al. 1979). The fact that the rainy season is more intense during the months with frequent mesoscale disturbances (Grist and Nicholson 2001; Nicholson and Grist 2000, manuscript submitted to *J. Climate*) suggests that the waves tend to enhance rainfall, as well as organize it.

In Grist (2002, hereafter Part I), the link between rainfall variability and wave activity was investigated using wavelet analysis. It was found that in wet years the AEWs tended to be stronger at the 600-mb level. The differences at 925 mb were less consistent. Here in Part II, we further investigate the relationship between wave activity and rainfall variability. To do this, four wet years of an extended wet period in the Sahel (1958–61) are contrasted with four dry years within an extended dry period (1982–85) (Fig. 1). The questions addressed are twofold: 1) are there observable differences in wave activity in the two sets of years, and 2) are differences in the basic state of the atmosphere in

---

* Current affiliation: James Rennel Division, Southampton Oceanography Centre, Southampton, United Kingdom.

Corresponding author address: Dr. Jeremy P. Grist, Room 254/16, James Rennell Division, Southampton Oceanography Centre, European Way, Southampton SO14 3ZH, United Kingdom.
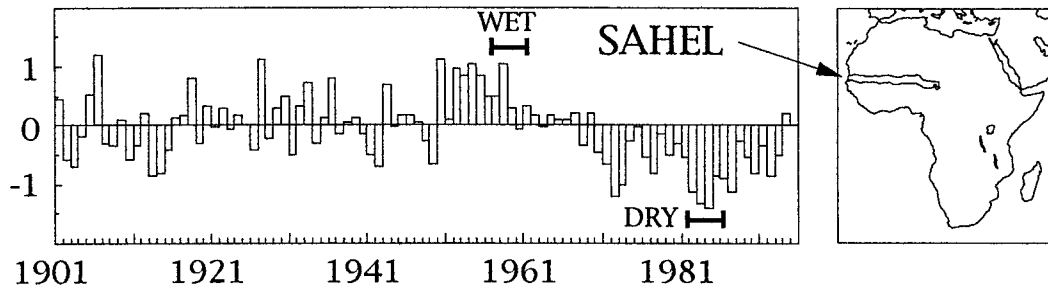E-mail: jyg@soc.soton.ac.uk

FIG. 1. Rainfall fluctuations in the African Sahel from 1901 to 1997, expressed as a regionally averaged standardized departure (departure from the long-term mean divided by the standard deviation).

the wet and dry years conducive to and consistent with the observed differences in wave activity? The former question is addressed using wavelet analysis, applied to National Centers for Environmental Prediction (NCEP) reanalysis data. The latter question is answered via an eigenanalysis using a linear instability model of the AEJ to assess the influence of the basic state on wave growth.

Because this study considers consecutive years within extended wet and dry periods, the work is more related to interdecadal variability than interannual. However, its conclusions will also have implications for interannual variability. The composite basic states corresponding to the wet years and dry years were determined by Grist and Nicholson (2001). The months of June through September, the rainy season over West Africa, are separately evaluated. The model predicts the magnitude of the perturbations and the wavelength of the most unstable mode. The model results are compared with various observations of rainfall and waves over West Africa.

This paper commences with an overview of the dynamical systems influencing West Africa. Then, in section 3, details of the dataset, wavelet analysis, and a brief overview of the model are presented. The characteristics of the two basic states are described in section 4. Further detail on the model and results of the eigenanalysis are presented in section 5. The results of the wavelet analysis and a comparison between model results and observations are presented in section 6. In section 7 dynamical aspects of the problem and an analysis of instability are presented. In our summary and conclusions (section 8), implications of this work for the general understanding of interannual and interdecadal variability over West Africa are described.

2. Overview of dynamical systems influencing West Africa

The rainfall field over West Africa is characterized by a zone of maximum precipitation that migrates north and south throughout the course of the year. This zone lies to the south of the surface position of the ITCZ and its seasonal excursion roughly parallels the seasonal ex-

cursion of the ITCZ. The rain belt comprises numerous disturbances that are dynamically linked to the midlevel AEJ. Westward-propagating mesoscale disturbances, termed cloud clusters, are the dominant convective system. Certain environment factors, such as vertical wind shear, buoyant energy, low-level jets, and latitude, determine whether convection is transformed into these long-lived and organized systems (Laing and Fritsch 1993). The frequency of cloud clusters and the amount of rainfall associated with them is modulated by transient synoptic-scale African or easterly waves (Houze and Betts 1981; Thompson et al. 1979).

These waves originate as a consequence of a joint baroclinic–barotropic instability associated with the vertical and horizontal shear of the midtropospheric AEJ. The waves, as well as the cloud clusters, are generally confined to a relatively narrow latitudinal zone near and south of the jet (Laing and Fritsch 1993; Norquist et al. 1977; Albignat and Reed 1980; Burpee 1972). This zone corresponds to the region between the axes of the AEJ and the upper-tropospheric tropical easterly jet (TEJ; Tourre 1981; Bounoua 1980). It is also straddled by the cores of the AEJ and a similar midtropospheric easterly jet in the Southern Hemisphere (Nicholson and Grist 2001). The growth and development of the waves are influenced by several factors, including Saharan dust (Karyampudi and Carlson 1988), the magnitude of the horizontal and vertical shear of the AEJ (e.g., Rennick 1981), and latent heat release (Norquist et al. 1977). A number of general circulation models have successfully simulated the waves (Reed et al. 1988; Druyan and Hall 1994, 1996; Xue and Shukla 1993; Thorncroft and Rowell 1998).

Both observations and models have shown that characteristics of the AEJ (particularly horizontal and vertical shear) and the mean zonal flow influence the characteristics of these waves (Burpee 1974; Simmons 1977; Mass 1979; Rennick 1976, 1981; Kwon 1989). During the wet 1950s, when the AEJ was relatively weak (Newell and Kidson 1984), the waves appear to have occurred at two discrete periodicities of approximately 2–3 and 4–6 days (Adefolalu 1974). The wave spectra for the early 1960s showed a single maximum at about 3–5 days (Burpee 1972); their longitudinal extent was also
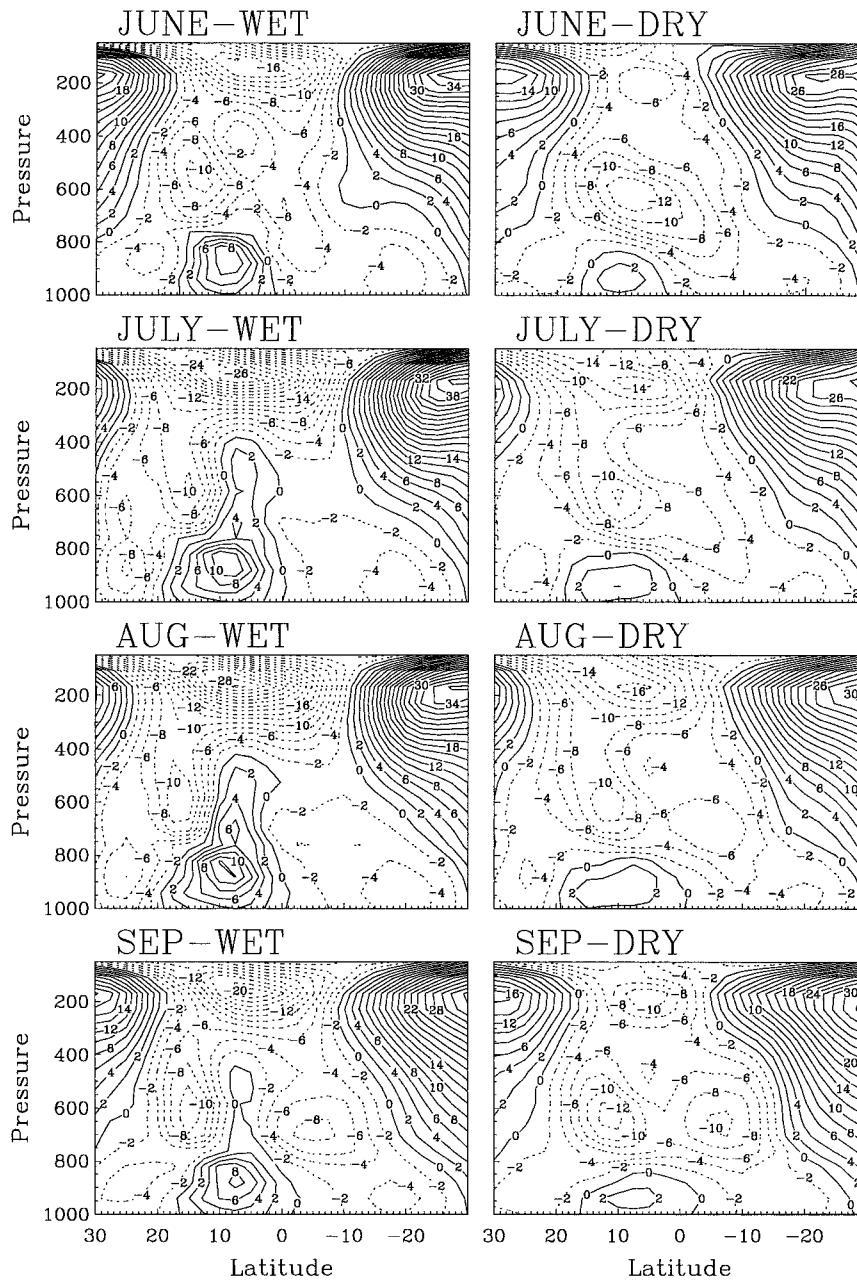
FIG. 2. Mean zonal wind speed (m s^{-1}) averaged between 10°W and 20°E. (left) Wet composite, 1958–61; (right) dry composite, 1982–85.

much smaller than during the wetter years. However, their relationship to the interannual variability of rainfall is unclear. There is evidence that they enhance rainfall, but the number traversing the West African coast systematically increased as rainfall decreased from the 1960s to the late 1970s (Reed 1988).

Both the shear instability and waves are present throughout the rainy season. However, rainfall is fairly localized in the first half of the season and the waves appear to contribute to the development of large-scale rainfall systems only later in the season (Reeves et al.

1979; Chen and Ogura 1982; Miller and Lindzen 1992). For the waves to organize rainfall, they must produce moisture convergence and be reasonably close to the moist layer. Past studies have suggested that in the Sahel, these prerequisites are present only in late summer. This fact may help to explain the contrast between the rainfall regimes in June–July and August–September, noted in several studies, and the fact that mesoscale convective complexes are much more frequent during the latter period (Laing and Fritsch 1993), when wave amplitude is larger (Duvel 1990).

3. Data and methodology

This study is a follow-up to Part I and Grist and Nicholson (2001), which relied heavily upon NCEP reanalysis project data (Kalnay et al. 1996). In the first study, Grist examined wave activity in 10 wet years and 10 dry years by applying wavelet analysis to NCEP 600-mb wind data at 15°N and 0°, in the central Sahel and relatively near the jet core. In the latter study, Grist and Nicholson examined characteristics of atmospheric circulation and rainfall for two composites corresponding to four wet years and four dry years, using NCEP data to evaluate atmospheric circulation and gauge data (see Nicholson et al. 2000) to evaluate the rainfall regime. Upper air data were further used to corroborate circulation contrasts noted in the NCEP dataset between the wet and dry year composites. The basic states of the wet and dry composites analyzed by Grist and Nicholson (2001) were used as input for the numerical model described in section 5.

Analysis of easterly wave activity

To study the African easterly waves, wavelet analysis was carried out on daily time series for each of the 40 years of the reanalysis. As in Part I, the time series utilized were 600-mb meridional winds at 15°N and 0°. The location was chosen because it represents a typical West African location where AEWs are found. The meridional wind was used because it is an indicator of wave amplitude. The Morlet wavelet was applied and the 1% significance level was calculated in accordance with Torrence and Compo (1998). The wavelet transforms describe how the magnitude and periodicity of the waves change through the course of the year.

Rather than present 40 different transforms, the following technique was used to extract the salient information. We examined the time series of wavelet moduli for the individual wavelet scales 3, 4, 5, and 6. These are referred to by their equivalent corresponding Fourier periods (3.75, 5, 6.25, and 7.5 days, respectively). For the time series of each year, the variance that was not significant above a background of red noise was removed from the signal. For the four relevant wavelet scales, these time series were used to produce the annual cycle of wavelet modulus at a monthly time interval. This was done for composites of the four wet years, the four dry years, and the 40-yr mean.

4. The basic state in wet and dry years over Sahelian Africa

a. Mean zonal winds

The main contrasts between the wet and dry basic states are summarized in Tables 1 and 2 of Grist and Nicholson (2001), to which the interested reader is referred. The most dramatic difference is in the equatorial westerlies, associated with the humid Atlantic air (Fig.

2). In the wet year composite these extend well into the midtroposphere (generally to 400 mb), but are limited to 850 mb and below in the dry year composite. In the wet years the equatorial westerlies are best developed between about 5° and 10°N, but are well developed in the lower atmosphere between about 18°N and 2°S. In the dry years, they span the same latitudinal extent in the lowest layers, but are extremely weak. The core speeds reach 10 m s^{-1} in wet years, with the maximum speeds and a distinct jet core at about 850 mb, but only 2 m s^{-1} in dry years, with the maximum near 900 or 950 mb.

Differences between the wet and dry composites are also apparent in the TEJ and AEJ. The TEJ reaches its maximum intensity in July and August in both composites and the location of its core, which is generally at 5°–8°N from June to September, is relatively stable. The jet is markedly stronger in the wet composite, with core speeds exceeding 20 m s^{-1} from June through September, compared to 8–16 m s^{-1} in the dry composite. In contrast to the TEJ, the AEJ is generally weaker and situated farther north during the wet years. Monthly mean core speeds generally reach 10 m s^{-1} during the wet years but 12 m s^{-1} in the dry years. The core is slightly lower in the dry years, lying near 600 mb, compared to about 500 mb during the wet years. During the dry year composite, the jet core migrates from about 7°N in June to 12°N in August and September. During the wet year composite, it migrates from 13°N in June to 17°N in August, retreating to 15°N in September.

In August and September a second midtropospheric jet core is also apparent in the Southern Hemisphere at roughly 5°–10°S in the dry composite. Its core lies near 5°S in August and speeds are about 6 m s^{-1}. In September its core lies near 7°S and speeds exceed 10 m s^{-1}. In the wet composite, this second jet is apparent in June and September and it is roughly 4° farther north than in the dry composite. In June its core lies near the equator and is quite weak, but in September, when the core near 6°S, speeds are in excess of 8 m s^{-1}.

b. Temperature and moisture fields

Figure 3 shows a vertical cross section of mean temperature in August for the four wet years and four dry years. There is a temperature maximum in the lower troposphere and a relatively strong temperature gradient around 10°–15°N. Although the vertical structure of the composites is similar, Grist and Nicholson (2001; in their Fig. 13) observed some differences in the horizontal temperature gradient. Specifically, at 850 mb, the maximum horizontal temperature gradient was slightly stronger in July through September of the wet years. This appears to be related to contrasts in the seasonal changes of the surface and atmospheric heating in the two sets of years (Grist and Nicholson 2001).

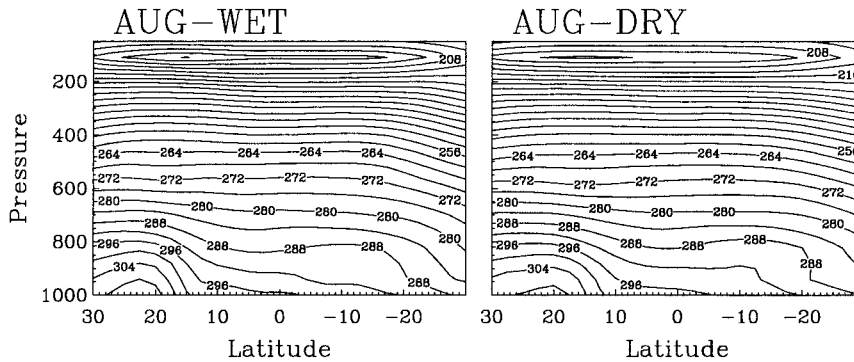Figure 4 shows a vertical cross section of mean rel-

FIG. 3. Vertical cross sections of mean temperature in Aug, averaged for the wet and dry composite in the sector 10°W–20°E.

ative humidity in August for the wet year composite, the dry year composite, and the difference between them. Apparent are three pronounced minima, corresponding to the lower troposphere over the Sahara, the subtropical westerly jet, and the tropical easterly jet. There is a strong maximum near the equator that extends into the midtroposphere. These features are evident in all months, but exhibit a pronounced seasonal shift. The main difference between the August wet and dry composites is a northward displacement of the equatorial maximum of relative humidity to roughly 13°N during August of wet years, compared to 6°N in the dry years. The relative humidity is also lower during the dry years, with the maximum reaching only about 74%, compared to 82% in the wet years.

5. The numerical model

The selection of the model was based on the following constraints: The model's basic state should account for the observed basic states prevailing during different months and different years in this region of Africa. These basic states should not be derived by means of analytical expressions, as done by several previous investigators, but rather should be based on observed data collected or interpolated at the pressure levels of the model. The model sophistication should match the present state of knowledge of the mechanisms one is trying to understand. It should be used primarily for understanding physical processes and mechanisms associated with the wet and dry years in the Sahel region.

The premise is that the alternation between wet and dry years is rooted in our understanding of the dynamics of the AEJ and its instabilities, the AEWs. The axis of this jet being near 15°N, quasigeostrophic (QG) dynamics is assumed adequate. If one were to associate distance traveled with the time taken for these instabilities to grow, the largest growth rates associated with the linear dynamics would adequately capture the dynamics near where the AEWs form and that linear QG framework would be sufficient.

The validity of the QG dynamics rests on the smallness of the Rossby number compared to unity, with values of about 0.10 used in midlatitudes. For the Coriolis parameter f_0 at 15°N, a length scale L_x about 1/5 of the most unstable AEW, and a jet speed of 10 m s^{-1}, we arrive at Rossby numbers of about 0.25; these numbers are still less than unity but larger than 0.10. As found by several previous authors in this and other contexts, linear theory provides valuable information even in regions of parameter space where it is not strictly valid.

a. Formulation of the model

A six pressure level, linear, adiabatic, quasigeostrophic model centered near 15°N was considered. It consists of the QG vertical vorticity equation;
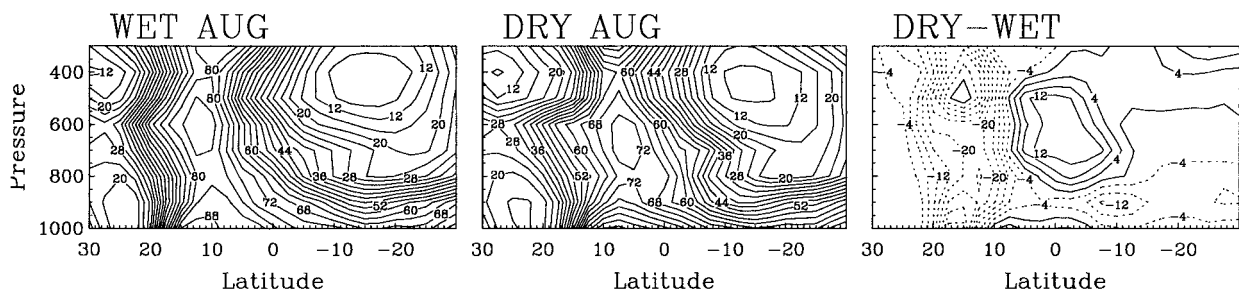
FIG. 4. Vertical cross sections of mean relative humidity in Aug, averaged for the wet and dry composites in the sector 10°W–20°E.

$$\frac{\partial}{\partial t}(\nabla^2\psi') + \overline{U}(y, p)\frac{\partial}{\partial x}(\nabla^2\psi') + \left(\beta - \frac{\partial^2\overline{U}}{\partial y^2}\right)\frac{\partial}{\partial x}\psi'$$

$$= f_0\frac{\partial\omega}{\partial p}, \qquad (1)$$

and the adiabatic thermodynamic equation;

$$\frac{\partial}{\partial t}\left(\frac{\partial\psi'}{\partial p}\right) + \overline{U}(y, p)\frac{\partial}{\partial x}\left(\frac{\partial\psi'}{\partial p}\right) - \frac{\partial\overline{U}}{\partial p}\left(\frac{\partial\psi'}{\partial x}\right) + S\omega = 0. \quad (2)$$

In these equations ψ' is the perturbation geostrophic streamfunction, ω is the perturbation vertical velocity in pressure coordinates, S is the background static stability taken as a function of p only, f_0 is the Coriolis parameter at 15°N, while β is the north–south derivative of that parameter at that latitude. The static stability, or stratification parameter, is

$$S = -\frac{RT}{p}\frac{d\ln\Theta}{dp}, \qquad (3)$$

where Θ is the background potential temperature and the other quantities have their standard meaning. The QG model requires the judicious selection of $S(p)$, which was taken as the horizontal average over a fairly broad region centered on the AEJ axis.

b. The eigenvalue problem and model verification

A normal mode solution is sought. The continuous equations (1) and (2) are finite differenced in pressure, resulting in a set of finite-difference equations for the vertical vorticity and the thermodynamics equations at their respective pressure levels. The radiation conditions are prescribed on the lateral boundaries (see Kwon 1989, p. 3622, for details) while the vertical velocity vanishes on both the lower and upper pressure levels of the model, $p = 1000$ and $p = 100$ mb. These boundary conditions result in an eigenvalue problem for the complex phase speed. The method of solution is similar to that described in Kwon (1989), who considered stability calculations of both dry and wet dynamics of the AEJ. He found very similar results in both cases. We note that it is the temperature and wind structures associated with the basic state that typify a dry year or a wet year.

The model performance was validated against the numerical integrations obtained by previous investigators. The stratification was set to a constant and two analytical expressions for the zonal wind flow were used to compare with the result reported by Kwon (1989). The shape of the numerically derived perturbation streamfunction both in the vertical and in pressure levels compared well with the results of both basic states used by Kwon (1989) and Simmons's (1977) basic state profile. Also the plot of the growth rates and phase speeds as a function of the horizontal wavenumber compared well with similar plots presented by these investigators.

c. Basic states of the model

The linear instability model we are using requires a basic state consisting of wind and temperature variables. Although the model is dry, the effects of moisture have been incorporated indirectly via the basic state winds. The basic states for June through August for mean zonal wind, temperature, and humidity are essentially those presented in Figs. 2 and 3, but with temperature converted to potential temperature. The four wet years are 1958, 1959, 1960, and 1961, and the four dry years are 1982, 1983, 1984, and 1985 (Fig. 1). NCEP data are interpolated onto the appropriate model levels.

The strongest contrast between the wet and dry states is evident in the zonal wind field. In both basic states a well-developed AEJ in the midtroposphere of the extratropical latitudes, a westerly flow in the lower troposphere, and a strong TEJ in the upper troposphere are evident. However, there are marked contrasts between the two basic states in the strength of the three easterly wind systems, in the depth of the westerly flow, and in the location of the AEJ.

d. Results of eigenanalysis of wet and dry basic states

Figure 5 shows the growth rate of waves for the wet and dry composites in the months of June through September. In the dry composite, the growth rate is relatively low during all four months and there is little difference between the months. The month of weakest wave activity appears to be September. The model shows considerably higher growth rates for the monthly basic states of the wet composite. The differences are relatively small for June, and largest for July and August.

In all cases, the most unstable wavelength is roughly 3000 km. Much longer wavelengths are unstable in the wet case compared to the dry case, but in the spirit of linear stability analysis one focuses only on the wavelength of the most unstable wave and on its growth rate. Figure 5 shows that the growth rate of the most unstable waves in June through September range from 0.25 to 0.35 day^{-1} in the dry years and 0.42 to 0.88 day^{-1} in the wet years, the most unstable waves occurring in August in both dry and wet years.

These results suggest that the waves are weaker during the dry years. Higher phase speeds (not shown) are also indicated for the wet basic state (Part I). This increase in phase speed may be due to the fact that the mean basic-state velocities, particularly those of the TEJ, are greater in the wet years than in the dry years.

6. Observed wave activity in the wet years and dry years

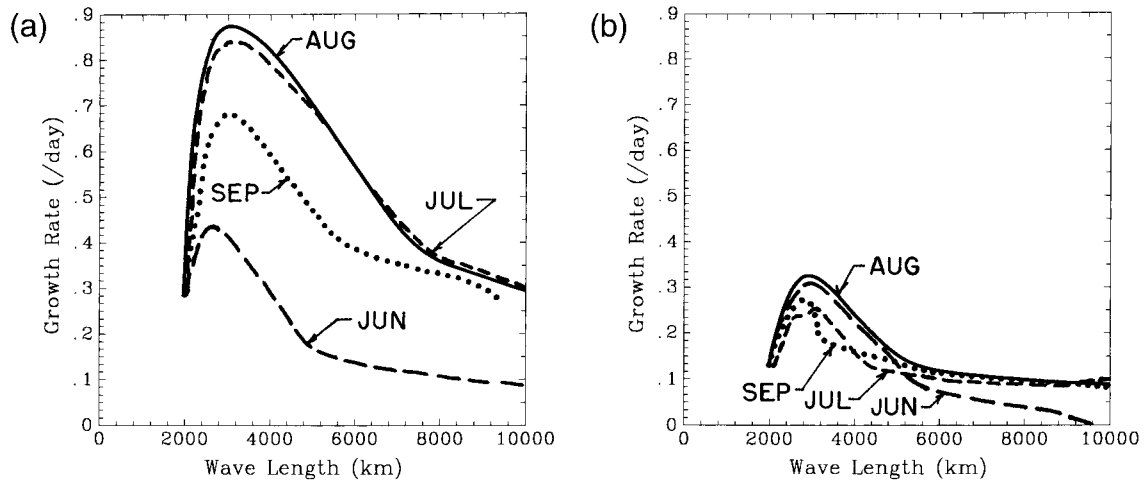Figure 6 shows the annual cycle of significant wavelet moduli. The information was calculated from the 40

FIG. 5. Wave growth derived from the different basic states, (left) the wet years (1958–61) and (right) dry years (1982–85).

wavelet transforms of the 600-mb v component. The values represent daily averages for each month. Wave activity is strong from June through September for Fourier periods of 3.75, 5.0, and 6.25 days and for August and September for the 7.5-day period. For most months and wave periodicities the wave amplitude is greater in wet years than in dry years. These differences are large for four out of the four Fourier periods in August, and for three out of the four Fourier periods in September. For periodicities of 3.75 days there is little difference in the wavelet modulus between the dry composite and the 40-yr mean, but for the wet composite the wave modulus is larger than the mean (i.e., the waves are stronger) from June through September. For periods of 5.0, 6.25, and 7.5 days, the wave modulus for the wet composite is greater than for the 40-yr mean, and the modulus for the dry composite is smaller than for the mean.

7. Discussion

a. Comparison of observational and theoretical results

Observational studies have shown variable wavelengths for the easterly waves over West Africa. Reed et al. (1977) found a range of 2000–5000 km, with a mean of 2500 km. Burpee (1972, 1974) suggested a range of 2000–4000 km. His spectral analysis of winds suggested a wavelength of 4000 km, but composite techniques suggested 3000 km. Our model results, with the most unstable wavelength being generally around 3000 km is in agreement with these observational studies. The studies of Burpee and those of Adefolalu (1974) also indicated that waves with a larger longitudinal extent (i.e., longer wavelengths) developed during the wetter years. Because phase speed is greater in wet years, the larger Fourier periods are associated with longer wavelengths. Thus the observation of longer wave-

lengths in wet years is consistent with both the wavelet analysis and the model eigenanalysis.

Another result of the model eigenanalysis, the greater growth rates in wet years, also compares favorably with observed differences in wave activity during wet and dry years. The faster growth rate in wet years could account for the more intense waves and increased wave activity in wet years, shown by the wavelet analysis in section 6.

The model results are interesting in view of the conclusion that for the Fourier periods of 7.5 days (the longer waves) disturbances become more prominent during the wet years. Lamb et al. (1998) found that the wetter years are associated with an increase in the number of large disturbances, with little change in the total number of rainfall events. Likewise, Nicholson (2000) showed that the difference between a "wet" and "dry" August appears to be one or more rainfall events that bring from 50 to 180 mm day^{-1}; no such events occurred during the dry years and the frequency of rainfall was otherwise similar in the wet and dry years. The more intense systems are likely to be associated with larger-scale disturbances, that is, longer waves.

The model results for June and September also provide an interesting comparison for observed differences in rainfall in wet and dry years. For June, the model indicates relatively little contrast in wave characteristics between the wet and the dry cases. Notably, there is relatively little contrast in June rainfall during the wet years and the dry years (Nicholson et al. 2000). For September, the model shows very low growth rates in the dry case, but markedly greater growth rates in the wet case. This is interesting in view of two observations based on gauge data: both the amount and intensity of September rainfall is greatly reduced during dry years (Grist and Nicholson 2001; Nicholson et al. 2000). These model results further imply that September plays a more prominent role in the rainy season in wet years than in dry years.
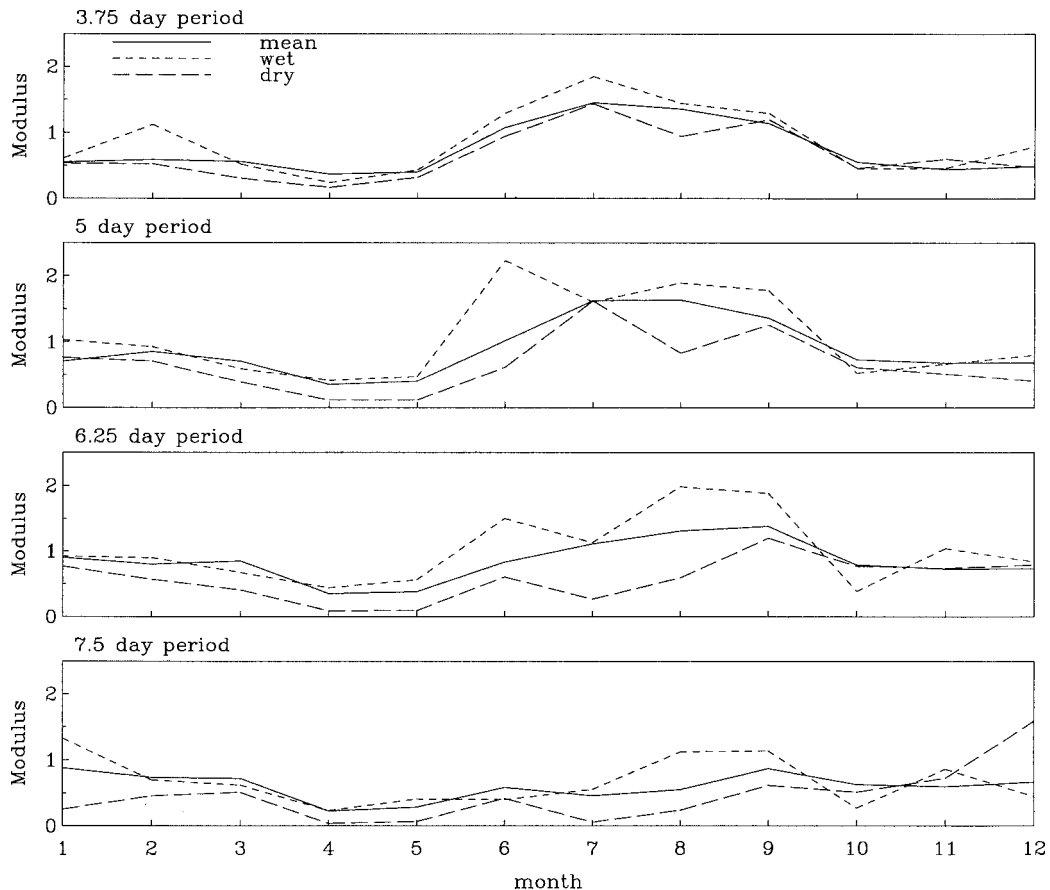
FIG. 6. Annual cycle of significant wavelet moduli for different Fourier periods at 600 mb. The values represent daily averages for each month. Solid line, 40-yr mean; short-dashed line, mean of four wet years; and long-dashed line, mean of four dry years.

The model results provide a favorable comparison with other aspects of observed wave activity. Figure 2 shows that in the dry composite, the basic state and the dynamic instabilities show little change during the course of the season and tend to resemble the June basic state of the wet years. The model shows that the basic state in these months is not conducive to wave growth. This is consistent with the observations that rainfall is fairly localized in the first half of the season (e.g., in Jun and early Jul) and that the waves appear to contribute to the development of large-scale rainfall systems only later in the season (Reeves et al. 1979; Chen and Ogura 1982; Miller and Lindzen 1992).

b. The links between waves, the AEJ, and dynamic instabilities

1) RECENT PRIOR STUDIES

It has long been established that both barotropic and baroclinic instabilities of the AEJ contribute to the generation of easterly waves (see Thorncroft and Hoskins 1994 and references within). However, it is not clear which is the dominant instability mechanism.

Part of the answer may lie in the fact that the instability mechanism appears to vary with latitude. The modeling study of Reed (1988) found two preferred regions of instability on either side of the AEJ. This was possible due to the strong dependence on the Coriolis parameter (Reed 1988). The observational work of Grist and Nicholson (2001) examined the distribution of vertical and horizontal shear in the wet and dry year composites. That study tentatively concluded that the dominant mechanism is probably baroclinic in the Sahel and barotropic farther south, consistent with Reed's conclusions. Thorncroft (1995), using a linear instability model, likewise showed contrasts in the energy conversions on a "desert jet" (analogous to a more northern jet) and a "shear jet" (analogous to a more southern jet). He similarly concluded that baroclinic was more important for the desert jet than for the shear jet, but he noted that barotropic instability was still dominant in both cases.

2) FURTHER DYNAMICAL IMPLICATIONS

The two model experiments and the four months included within them assign varying degrees of baroclinic

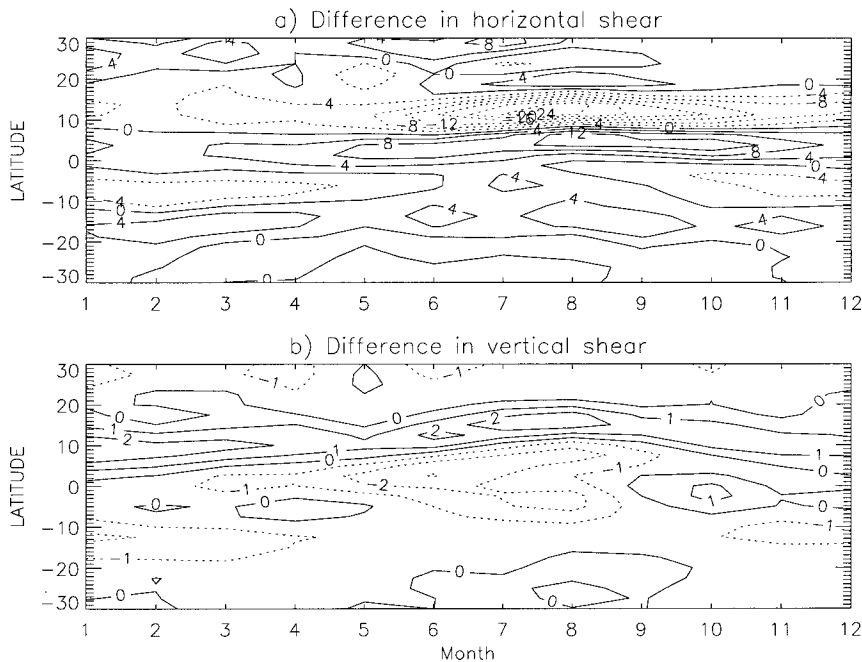## a) Difference in horizontal shear

b) Difference in vertical shear

FIG. 7. Difference in (a) horizontal shear and (b) vertical shear (10°W–20°E) between wet and dry years, as a function of latitude and month. The units for horizontal shear are 10^{-6} s^{-1} and the units for vertical shear are 10^{-4} m s^{-1} Pa^{-1}.

and barotropic instability. The horizontal and vertical shear associated with these basic states illustrate this to some degree. Figure 7 shows the difference in horizontal and vertical shear between wet and dry years. To the south of 10°N, the horizontal shear, which is related to barotropic instability, is markedly weaker in the dry composite than in the wet composite. The vertical shear, which is related to baroclinic instability, shows less contrast between the two composites, but it is noticeably weaker at around 10°N in dry years.

Because the latitudinal location of the shear zones shift toward the equator in the dry composite, the magnitudes of the shears alone do not give a full picture of the contrasts in the instability in the eight eigenanalysis in Fig. 5. The global analyses of Charney and Stern (1962) provide additional verification and validation of the two methods previously discussed. This analysis requires the assumptions that 1) the AEJ can be treated as an internal jet, 2) the zonal wind is quasigeostrophic, 3) the monthly means are roughly representative of the instantaneous state of the jet, and 4) that the flow is inviscid and adiabatic. The first assumption is not strictly true, as it requires that the waves be insignificant at the surface. Although the waves are evident at the surface, the initial perturbation is at midlevels, so that the assumption is approximately true during the early growth phase of the wave. The successful simulation of the AEJ and easterly waves by quasigeostrophic models (e.g., Kwon 1989; Thorncroft and Hoskins 1994; Thorncroft 1995) validates the second assumption. An analysis in Grist and Nicholson (2001), showing that the

day-to-day variations in the core speed of the jet are relatively small, justifies the third assumption. The inviscid, dry model stability analyses compare favorably with observations, thereby justifying the fourth assumption.

Charney and Stern (1962) addressed the problem of ascertaining whether an internal jet with horizontal and vertical shear (such as the AEJ) is unstable, and thus capable of producing disturbances. Considering the disturbances associated with the "polar night jet" (which is somewhat analogous to the AEJ) to be of the same order as the Rossby radius of deformation, they used the quasigeostrophic potential vorticity equation:

$$\left(\frac{\partial}{\partial t} + \mathbf{v} \cdot \mathbf{\nabla}_p\right)\left[\nabla_p^2\psi + f + \frac{\partial}{\partial p}\left(\frac{f_0^2}{S}\frac{\partial \psi}{\partial p}\right)\right] = 0. \quad (4)$$

The geostrophic streamfunction is defined as $\psi \equiv gz/f_0$. Vorticity is expressed in the form $\zeta = \nabla_p^2\psi$. This equation expresses the conservation of quasigeostrophic vorticity. Assuming infinitesimal perturbations superimposed on a basic-state zonal wind field $\overline{U}(y,p)$, in thermal wind equilibrium with the pressure and temperature fields, the equation is linearized:

$$\left(\frac{\partial}{\partial t} + \overline{U}\frac{\partial}{\partial x}\right)\left[\frac{\partial^2 \psi'}{\partial x^2} + \frac{\partial^2 \psi'}{\partial y^2} + f_0^2\frac{\partial}{\partial p}\left(\frac{1}{S}\frac{\partial \psi'}{\partial p}\right)\right] + \frac{\partial \psi'}{\partial x}\frac{\partial \overline{q}}{\partial y}$$
$$= 0. \quad (5)$$

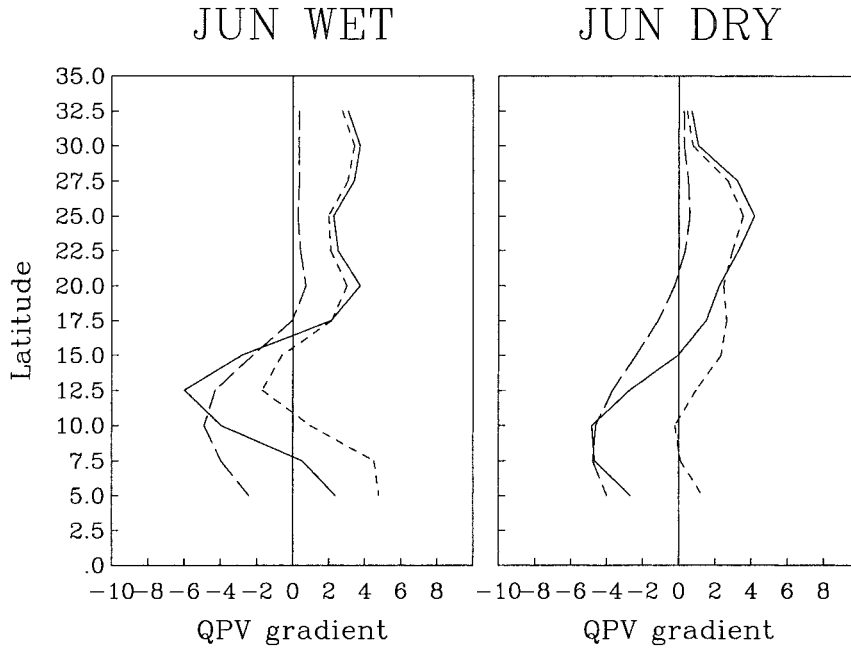The bar designates a zonal mean, and the prime a de-

FIG. 8. Quasigeostrophic potential vorticity gradient at 600 mb (10°W–20°E) as a function of latitude, for Jun (left) wet and (right) dry years. Solid line, total QGPV gradient; short-dashed line, barotropic term; and long-dashed line, baroclinic term. Units are 10^{-11} s^{-1}.

parture from this mean. The basic state of quasigeostrophic vorticity is

$$\overline{q} = f + \frac{\partial^2 \overline{\psi}}{\partial y^2} + f_0^2 \frac{\partial}{\partial p}\left(\frac{1}{S}\frac{\partial \overline{\psi}}{\partial p}\right). \qquad (6)$$

The quasigeostrophic potential vorticity (QGPV) gradient can be broken down into a term that is associated with vertical shear (baroclinic instability) and a term that is due to horizontal shear (barotropic instability):

$$\frac{\partial \overline{q}}{\partial y} \equiv \underbrace{\beta - \frac{\partial^2 \overline{U}}{\partial y^2}}_{\text{barotropic}} - \underbrace{f_0^2 \frac{\partial}{\partial p}\left(\frac{1}{S}\frac{\partial \overline{U}}{\partial p}\right)}_{\text{baroclinic}}. \qquad (7)$$

It can be shown that for the solution of (5) to have an imaginary part and the wave to grow exponentially, $\partial \overline{q}/\partial y$ must change sign somewhere in the domain. Charney (1973) showed that for tropical North Africa, where the flow is easterly and the temperature increases with latitude, $\partial \overline{q}/\partial y$ must become negative somewhere in the domain for there to be instability. Burpee (1972) computed (7) from mean monthly values of radiosonde observations for August 1957–64. He showed that $\partial \overline{q}/\partial y$ did become negative, thus implying that the August mean state was dynamically unstable. The vertical and the horizontal shears were of similar importance in ensuring that the necessary condition for instability was met.

The QGPV gradient was calculated at the 600-mb level. The zonal averages $U(y, p)$ and $\theta(y, p)$ at 500,

600, and 700 mb were taken from our wet and dry basic states. The density of air (ρ) at 600 mb was taken from a table of the mean tropical atmosphere (Jordan 1958). Beta and the Coriolis parameter were taken as constants at the center of the region.

Figures 8–11 show the total QGPV gradient, the baroclinic term, and the barotropic term in Eq. (7) for June through September, respectively, of wet and dry basic states shown in Figs. 2, 3, and 4. Clearly, in each case the gradient becomes negative somewhere within the subtropical latitudes. This is the principal factor in instability (Thorncroft and Hoskins 1994). Also, the quantitative values of the total QGPV gradient and the individual baroclinic and barotropic terms can serve as a first approximation for the degree of instability and the relative contribution of the two mechanisms.

Thus, the fact that the total QGPV gradient is much more strongly negative in the wet years (Figs. 8–11) implies a potentially greater instability in the wet years than in the dry years. The maximum negative gradient shifts seasonally, attaining a maximum northward position in August, and it is farther north in the wet years than in the dry years. This is consistent with the seasonal movement of the AEJ and tropical rainbelt, and the southward displacement of these features in dry years (Grist and Nicholson 2001). The barotropic term also tends to become more dominant as the rainy season progresses, consistent with conclusions of Grist and Nicholson.

The relative contributions of the baroclinic and barotropic terms to the QGPV gradient contrast strongly
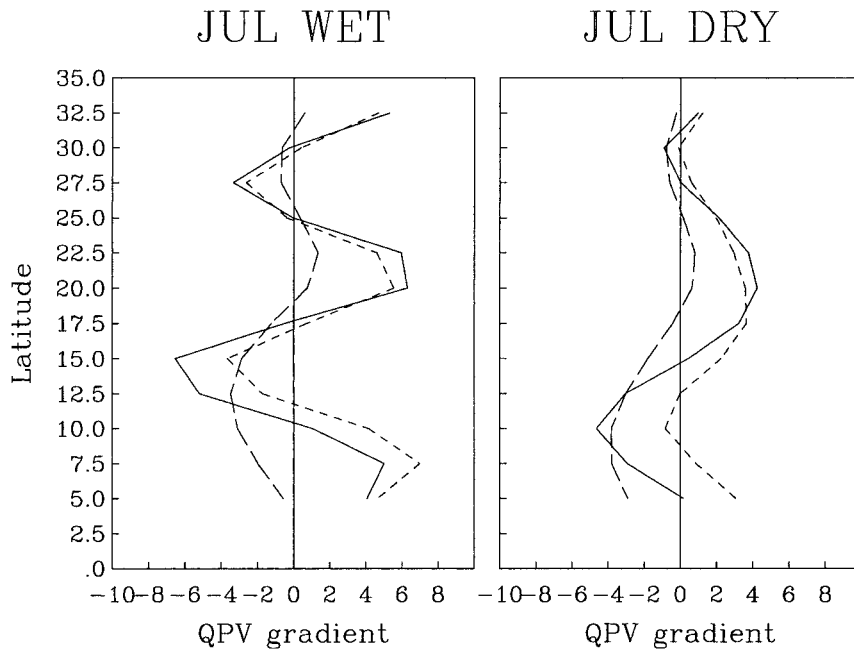
JUL WET   JUL DRY

FIG. 9. Quasigeostrophic potential vorticity gradient at 600 mb (10°W–20°E) as a function of latitude, for Jul (left) wet and (right) dry years. Solid line, total QGPV gradient; short-dashed line, barotropic term; and long-dashed line, baroclinic term. Units are 10^{-11} s^{-1}.

in wet and dry years. Except for June, the barotropic term is considerably greater in the wet years than in the dry years. Grist and Nicholson (2001) similarly observed that the horizontal wind shear is much greater in the wet years than in the dry years, except for June.

Again except for June, the barotropic term is considerably greater than the baroclinic term in the wet years, but the terms are of roughly equal magnitude in the dry years. The baroclinic term does not show any marked contrast between wet and dry years and it is greater in
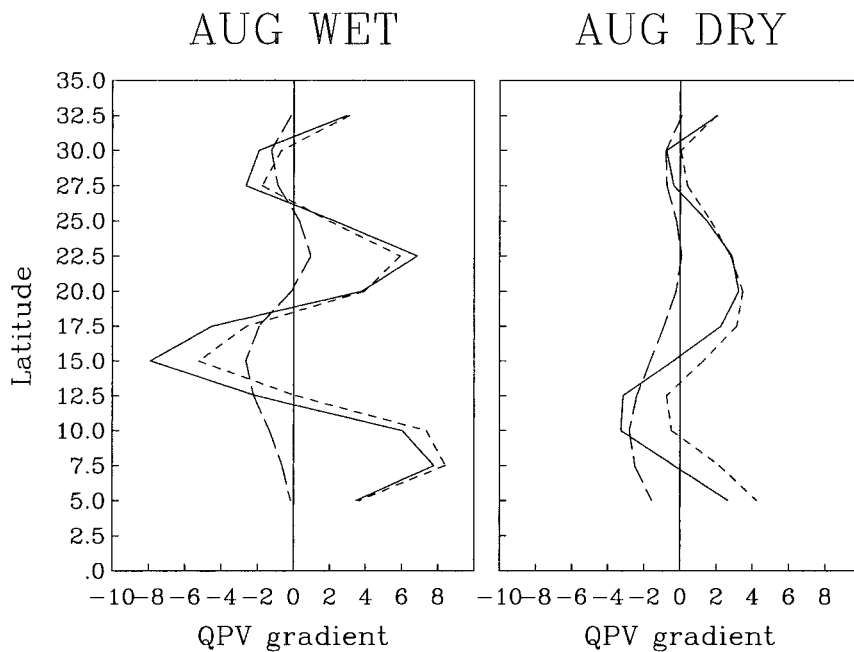
AUG WET   AUG DRY

FIG. 10. Quasigeostrophic potential vorticity gradient at 600 mb (10°W–20°E) as a function of latitude, for Aug (left) wet and (right) dry years. Solid line, total QGPV gradient; short-dashed line, barotropic term; and long-dashed line, baroclinic term. Units are 10^{-11} s^{-1}.

SEP WET SEP DRY

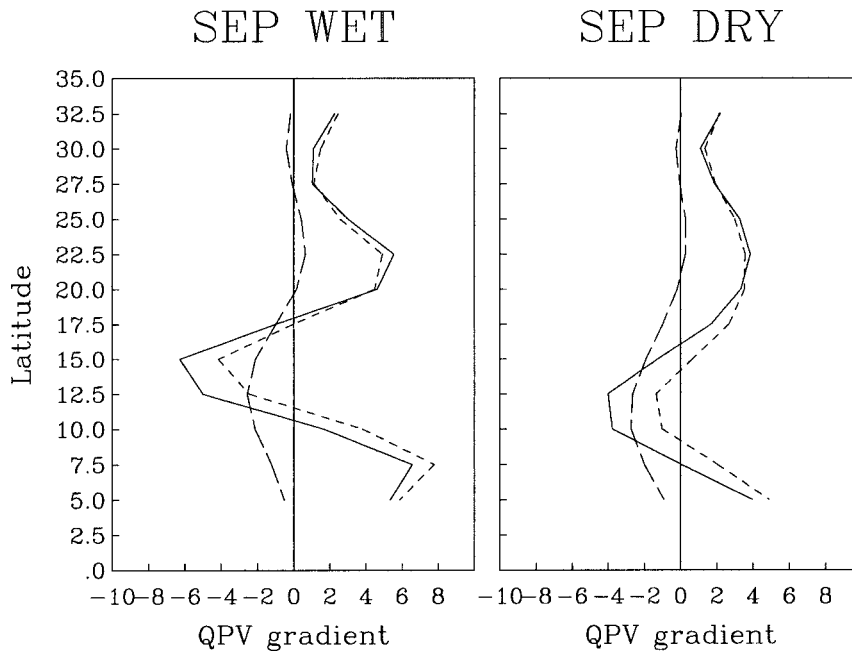

FIG. 11. Quasigeostrophic potential vorticity gradient at 600 mb (10°W–20°E) as a function of latitude, for Sep (left) wet and (right) dry years. Solid line, total QGPV gradient; short-dashed line, barotropic term; and long-dashed line, baroclinic term. Units are 10^{-11} s^{-1}.

June and July than in August and September. This is likewise consistent with the patterns of vertical wind shear noted by Grist and Nicholson.

A final observation concerns the relative importance of baroclinic versus barotropic instability over the Sahel. Grist and Nicholson (2001) had concluded that baroclinic instability is the dominant mechanism over the Sahel, with barotropic instability being dominant in the region farther south (south of the jet core). That preliminary conclusion was based solely on the patterns of horizontal and vertical shear. The more complete analysis presented here in Figs. 8–11 suggests that barotropic instability is dominant in both locations, but that baroclinic instability plays a greater role in the Sahel than farther south. This is in agreement with the results of Thorncroft (1995). Figures 8–11 also indicate, in agreement with conclusions based on shear alone, that the baroclinic instability is present in the Sahelian latitudes during the wet years, but not in the dry years, when the patterns are all shifted southward. Thus baroclinic instability probably plays a role in the interannual variability in the Sahel, but not in the latitudes south of the Sahel. More definitive conclusions on the importance of these instability mechanisms require an energetics analysis.

Relating the instability analysis in Figs. 8–11 to the model results in Fig. 5, it is relevant to examine the main contrasts between the basic states that produce large growth rates of waves and numerous unstable modes and those that do not. The larger growth rates occur in July through September of the wet years; small-

er growth rates occur in June of both composites and July through September of dry years. In the relatively unstable basic states of the three wet months, the baroclinic term is markedly dominant. In the states with potentially greatest instability (Jul and Aug), both barotropic and baroclinic terms are relatively strong. In the less stable basic state of wet Septembers, the baroclinic term is strong only in the latitudes well south of the maximum QGPV gradient where the barotropic term is relatively small. In the five comparatively stable basic states of June and dry July, August, and September, the barotropic and baroclinic terms are of comparable magnitude. The overall conclusion to be drawn from this is that both the barotropic and baroclinic terms are important and that the relative magnitude of the two plays a substantial role in wave growth. This is consistent with the conclusions of Rennick (1981), based on a linear instability model of the AEJ. This also underscores the complexity of the wave growth and its relationship to the basic state.

8. Summary and conclusions

This study has identified contrasts in wave activity over West Africa between wet years and dry years. In general, the waves are more intense in the wet years. Wave activity in the dry years shows little contrast with the long-term mean, suggesting that changes in wave activity are associated with anomalously wet conditions in the region, but play a lesser role in producing anom-

alously dry conditions. The analysis also indicated a broader range of wave periods during the wet years.

This study has shown, via a numerical model, that the contrasting dynamics of the wet and dry basic states of the atmosphere strongly modify the character of wave perturbations. The simulated changes are consistent with observations, particularly the weaker wave growth in the dry years. The model suggested that the biggest contrast would be apparent in September, the smallest in June. This is consistent with contrasts evident in the rainfall regime in wet and dry years. During the wet years in the Sahel, very little change in rainfall is apparent in June, the first month of the rainy season. September, the last month of the rainy season, shows marked contrast in both the amount and intensity of rainfall in the wet and dry years.

Earlier studies failed to show clear-cut relationships between wave activity and the interannual variability of rainfall. Goldenberg and Shapiro (1996), for example, concluded that differences in wave characteristics between wet and dry years had not been well established. Similarly, Reed (1988) showed that the number traversing the West African coast systematically increased as rainfall decreased from the 1960s to the late 1970s. Our study has shown systematic differences in wave activity in the wet and dry years and has produced results that help to explain the conclusions of earlier papers.

Our work, both the wavelet analysis and the model, also suggests AEWs are more intense in wet years. This is consistent with findings (e.g., Lamb et al. 1998; Nicholson 2000) showing that in wetter years there are more intense rainfall events, rather than a greater number of events. One or two very large disturbances can account for much of the difference between a ''wet'' August and a ''dry'' August in the Sahel. Thus, even if a direct link between rainfall events and waves is assumed, a correlation between the number of waves and the character of the rainy season would not necessarily be expected. Rather a slight increase in the number of intense wave disturbances might be expected.

A conceptual model developed by Nicholson and Grist (2001, manuscript submitted to *Int. J. Climatol.*) for understanding the interannual variability of Sahel rainfall can further provide an explanation for some of the results in the current paper. In this paradigm, the shift between the wet years in the Sahel prior to 1968 and the subsequent dry years is produced by a pronounced equatorward displacement of the AEJ. This displaced the core of the tropical rainbelt to latitudes south of the Sahel, that is, into the region termed the Guinea coast. As the current paper also shows, this meridional shift of the AEJ and other associated changes in the shear of the basic state markedly altered the prevailing dynamical instabilities. However, once the AEJ moved to its more equatorward position, there was little contrast in atmospheric circulation or dynamical instabilities between those years in which the rainbelt was

relatively intense (and hence the Guinea coast wet) and those in which the rainbelt was weakly developed (and the Guinea coast was dry). It was also noted by numerous papers that the tropical teleconnections to rainfall (e.g., links to SSTs, ENSO, etc.) are different between the years before and after 1968 (Semazzi et al. 1988; Ward 1998; Janicot et al. 1996, 2000, manuscript submitted to *Climate Dyn.*; Trzaska et al. 1996; Rowell 2001), consistent with the altered dynamics.

A synthesis of those prior results with the ones presented in the current paper suggests the following link between interannual variability and wave activity. It suggests that the wet basic state, especially the northward displacement of the AEJ and the enhanced shear due to intense equatorial westerlies, led to enhanced wave activity that likely served to enhance rainfall and extend the length of the rainy season. The dry basic state is less conducive to wave activity and changes of wave activity do not appear to modulate seasonal rainfall in that state. On the other hand, in this state the atmosphere appears to be more sensitive to external forcing (such as ENSO and SSTs). However, the specific factors that contribute to interannual variability in this state have not been explicitly identified. Factors such as characteristics of the moist layer or the position and/or intensity of the ITCZ may play a role.

Thus, contrasting dynamics of the wet and dry basic states appear to influence the development of waves and the influence of external factors on West African rainfall. Knowledge of this dynamic dichotomy in the region may facilitate the improvement of seasonal forecasts of rainfall and hurricane activity, which is related to the waves.

REFERENCES

Adefolalu, D. O., 1974: The lower atmospheric summer easterly perturbation in tropical West Africa. Ph.D. thesis, The Florida State University, 276 pp.

Albignat, J. P., and R. J. Reed, 1980: The origin of African wave disturbances during phase III of GATE. *Mon. Wea. Rev.,* **108,** 1827–1839.

Bounoua, L., 1980: Relation enre champ de vent, genèse et propagation des lignes de grains ouest africaines. Mémoire de fin d'étude pour le diplome d'ingenieur d'eta de la Meteorologie, 108 pp. [Available from IHFR, BP 7019, Seddikia, Oran, Algeria.]

Burpee, R. W., 1972: The origin and structure of easterly waves in the lower troposphere. *J. Atmos. Sci.,* **29,** 77–90.

——, 1974: Characteristics of North Africa easterly waves during the summers of 1968 and 1969. *J. Atmos. Sci.,* **31,** 1556–1570.

Charney, J. G., 1973: Planetary fluid dynamics. *Dynamic Meteorology,* P. Morel, Ed., D. Reidel, 97–352.

——, and M. E. Stern, 1962: On the stability of internal baroclinic jets in a rotating atmosphere. *J. Atmos. Sci.,* **19,** 159–172.

Chen, Y., and Y. Ogura, 1982: Modulation of convective activity by large-scale flow patterns observed in GATE. *J. Atmos. Sci.,* **39,** 1260–1279.

Druyan, L., and T. Hall, 1994: Studies of African wave disturbances with the GISS GCM. *J. Climate,* **7,** 262–276.

——, and ——, 1996: The sensitivity of African wave disturbances to remote forcing. *J. Appl. Meteor.,* **35,** 1100–1110.

Duvel, J. P., 1990: Convection over tropical Africa and the Atlantic Ocean during northern summer. Part II: Modulation by easterly waves. *Mon. Wea. Rev.,* **118,** 1855–1868.

Goldenberg, S. B., and L. J. Shapiro, 1996: Physical mechanisms for the association of El Niño and West African rainfall with Atlantic major hurricane activity. *J. Climate,* **9,** 1169–1187.

Grist, J. P., 2002: Easterly waves over Africa. Part I: The seasonal cycle and contrasts between wet and dry years. *Mon. Wea. Rev.* **130,** 197–211.

——, and S. E. Nicholson, 2001: A study of the dynamic factors influencing the interannual variability of rainfall in the West African Sahel. *J. Climate,* **14,** 1337–1359.

Houze, R. A., Jr., and A. K. Betts, 1981: Convection in GATE. *Rev. Geophys. Space Phys.,* **19,** 541–576.

Janicot, S., V. Moron, and B. Fontaine, 1996: Sahel droughts and MENSO dynamics. *Geophys. Res. Lett.,* **23,** 515–518.

Jordan, C. L., 1958: Mean soundings for the West Indies area. *J. Meteor.,* **15,** 91–97.

Kalnay, E., and Coauthors, 1996: The NCEP/NCAR 40-Year Reanalysis Project. *Bull. Amer. Meteor. Soc.,* **77,** 437–471.

Karyampudi, V., and T. Carlson, 1988: Analysis of numerical simulations of the Saharan air layer and its effects on easterly wave disturbances. *J. Atmos. Sci.,* **45,** 3102–3136.

Kwon, H. J., 1989: A reexamination of the genesis of African waves. *J. Atmos. Sci.,* **46,** 3621–3631.

Laing, A., and J. M. Fritsch, 1993: Mesoscale convective complexes in Africa. *Mon. Wea. Rev.,* **121,** 2254–2263.

Lamb, P. J., M. A. Bell, and J. D. Finch, 1998: Variability of Sahelian disturbance lines and rainfall during 1951–1987. *Water Resources Variability in Africa during the XXth Century,* E. Servat et al., Eds., IAHS Publ. 252, 19–26.

Mass, C., 1979: A linear primitive equation model of African wave disturbances. *J. Atmos. Sci.,* **36,** 2075–2092.

Miller, R. L., and R. Lindzen, 1992: Organization of rainfall by an unstable jet with an application to African waves. *J. Atmos. Sci.,* **49,** 1523–1540.

Newell, R. E., and J. W. Kidson, 1984: African mean wind changes between Sahelian wet and dry periods. *J. Climatol.,* **4,** 1–7.

Nicholson, S. E., 2000: Land surface processes and Sahel climate. *Rev. Geophys.,* **38,** 117–139.

——, B. Some, and B. Kone, 2000: A note on recent rainfall conditions in West Africa, including the rainy season of the 1997 ENSO year. *J. Climate,* **13,** 2628–2640.

Norquist, D. C., E. E. Recker, and R. J. Reed, 1977: The energetics of African wave disturbances as observed during Phase III of GATE. *Mon. Wea. Rev.,* **105,** 334–342.

Reed, R., 1988: On understanding the meteorological causes of Sahelian drought. Persistent meteo-oceanographic anomalies and teleconnections. *Pontificae Academiae Scientiarum Scripta Varia,* C. Chagas and G. Puppi, Eds., Pontifical Academy of Science, 180–212.

——, D. Norquist, and E. Recker, 1977: The structure and properties of African wave disturbances as observed during phase III of GATE. *Mon. Wea. Rev.,* **105,** 413–420.

——, A. Hollingsworth, W. Heckley, and F. Delsol, 1988: An evaluation of the performance of the ECMWF operational system in analyzing and forecasting easterly wave disturbances over Africa and the tropical Atlantic. *Mon. Wea. Rev.,* **116,** 824–865.

Reeves, R., C. Ropelewski, and M. Hudlow, 1979: Relationships between large-scale motion and convective precipitation during GATE. *Mon. Wea. Rev.,* **107,** 1154–1168.

Rennick, M. A., 1976: The generation of African waves. *J. Atmos. Sci.,* **33,** 1955–1969.

——, 1981: Some sensitivity experiments with an African wave model. *J. Atmos. Sci.,* **38,** 106–113.

Rowell, D. P., 2001: Teleconnections between the tropical Pacific and the Sahel. *Quart. J. Roy. Meteor. Soc.,* **127B,** 1683–1706.

Semazzi, F. H. M., V. Mehta, and Y. C. Sud, 1988: An investigation of the relationship between sub-Saharan rainfall and global sea surface temperatures. *Atmos.–Ocean,* **26,** 118–138.

Simmons, A. J., 1977: A note on the instability of the African easterly jet. *J. Atmos. Sci.,* **34,** 1670–1674.

Thompson, R. M., Jr., S. W. Payne, E. E. Recker, and R. J. Reed, 1979: Structure and properties of synoptic-scale wave disturbances in the intertropical convergence zone of the eastern Atlantic. *J. Atmos. Sci.,* **36,** 53–72.

Thorncroft, C. D., 1995: An idealized study of African easterly waves. III: More realistic basic states. *Quart. J. Roy. Meteor. Soc.,* **121,** 1589–1614.

——, and B. J. Hoskins, 1994: An idealized study of African easterly waves. I: A linear view. *Quart. J. Roy. Meteor. Soc.,* **120,** 953–982.

——, and D. P. Rowell, 1998: Interannual variability of African wave activity in a general circulation model. *Int. J. Climatol.,* **18,** 1305–1323.

Torrence, C., and G. P. Compo, 1998: A practical guide to wavelet analysis. *Bull. Amer. Meteor. Soc.,* **79,** 61–78.

Tourre, Y., 1981: The squall line over West Africa and the tropical eastern Atlantic Ocean during GATE. Ph.D. dissertation, University of Virginia, 147 pp.

Trzaska, S., V. Moron, and B. Fontaine, 1996: Global atmospheric response to specific linear combinations of the main SST modes. Part I: Numerical experiments and preliminary results. *Ann. Geophys.,* **14,** 1066–1077.

Ward, M. N., 1998: Diagnostic and short-lead time prediction of summer rainfall in tropical North Africa at interannual and multidecadal timescales. *J. Climate,* **11,** 3167–3191.

Xue, J., and J. Shukla, 1993: The influence of land surface properties on Sahel climate. Part I: Desertification. *J. Climate,* **6,** 2232–2245.